

Quantifying Homo- and Heteromolecular Hydrogen Bonds as a Guide for Adduct Formation

Amit Delori,^[a] Peter T. A. Galek,^[b] Elna Pidcock,^[b] and William Jones*^[a]

Abstract: An investigation into the predictability of molecular adduct formation is presented by using the approach of hydrogen bond propensity. Along with the predictions, crystallisation reactions (**1a–1j**) were carried out between the anti-malarial drug pyrimethamine (**1**) and the acids oxalic (**a**), malonic (**b**), acetylenedicarboxylic (**c**), adipic (**d**), pimelic (**e**), suberic (**f**), azelaic acids (**g**), as well as hexachlorobenzene (**h**), 1,4-diiodobenzene (**i**), and

1,4-diiodotetrafluorobenzene (**j**); seven (**1a to 1g**) of these successfully formed salts. Five of these seven salts were found to be either hydrated or solvated. Hydrogen bond propensity calculations predict that hydrogen bonds be-

tween **1** and acids **a–g** are more likely to form rather than the H bonds involved in self-association, providing a rationale for the observation of the seven new salts. In contrast, propensity of hydrogen bonds between **1** and **h–j** is much smaller as compared to other bonds predicted for self-association/solvate formation, in agreement with the observed unsuccessful reactions.

Keywords: computer chemistry · cocrystallization · hydrogen bonds · knowledge-based predictions · pharmaceutical materials

Introduction

Molecular adducts (e.g., salts and co-crystals) are considered as alternatives when the physicochemical properties of a parent drug molecule are unsuitable or inadequate for satisfactory formulation.^[1] Considerable variation in such pharmaceutically important physical properties as solubility,^[2] dissolution rate,^[2] bioavailability,^[3] melting point,^[2h,4] stability^[5] and tableting properties^[6] can be achieved by such salt or co-crystal formation. The synthesis of pharmaceutical salts and co-crystals can, however, be difficult, especially if the drug molecule lacks strong hydrogen bond donor and/or acceptor functionality.^[7] Competition with solvate formation is also a factor that can influence the outcome. Frequently, supramolecular chemists rely on their experience and empirical knowledge for the judicious choice of an appropriate counter molecule or ion, and the Cambridge Structural Database (CSD) can be queried for specific, informative, examples.

Supramolecular chemists, especially those working with complex drug molecules in the pharmaceutical industry, would benefit from being able to predict the likelihood of

successes or failures in salt or co-crystal formation in order to suggest or prioritise experimental work more effectively. Identifying when solvate formation would be the likely outcome would also be beneficial.

Molecular adducts involving multiple neutral species, so-called co-crystals, are of particular current interest.^[1a] A difficulty, however, is a generally low success rate of co-crystallisation reactions making co-crystal screening a time-consuming process. Several strategies have been developed for choosing appropriate counter molecules (coformers). Hunter and co-workers have proposed a computational method for co-crystal screening,^[8] and Price and colleagues proposed difference in lattice energy of adduct and reactants as a criteria for predicting adduct formation.^[9] Additionally, Fábíán and co-workers proposed that coformers chosen based upon similarity in shape descriptors can increase the success of a co-crystallisation reaction.^[10]

To date the supramolecular synthon approach is the most widely used guide for the formation of salts or co-crystals.^[11] This approach suggests that molecules with complementary functional groups can interact to form an adduct. This synthon approach can, however, be less applicable in cases of multi-functional molecules,^[12] which are frequently of interest to the pharmaceutical industry. The synthon approach is qualitative in nature, takes into consideration only the complementarity of the functional groups and neglects other important factors, such as steric effects,^[13] which can prove vital for the effectiveness of a given interaction. The Cambridge Crystallographic Data Centre has developed a hydrogen bond propensity tool^[13b,14] that can be applied to predict the possibility of new polymorphs or adducts based on the potential H bonds that might form. On providing information of molecular structure, the software searches the CSD

[a] Dr. A. Delori, Prof. W. Jones
Department of Chemistry, University of Cambridge
Cambridge, CB2 1EW (UK)
Fax: (+44) 1223-336-017
E-mail: wj10@cam.ac.uk

[b] Dr. P. T. A. Galek, Dr. E. Pidcock
Cambridge Crystallographic Data Centre
12 Union Road, Cambridge, CB2 1EZ (UK)

Supporting information for this article is available on the WWW under <http://dx.doi.org/10.1002/chem.201103129>.

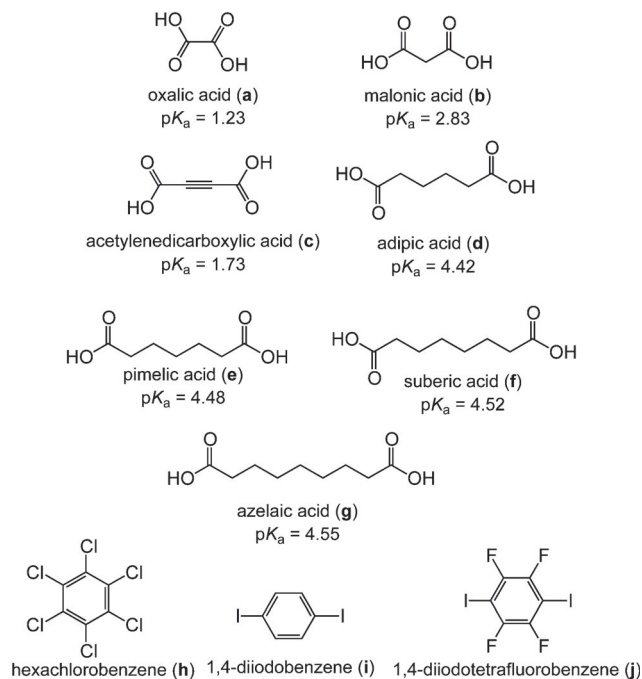
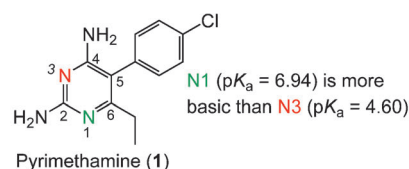
for those molecules/salts/co-crystals that have similar functional groups and quantifies the propensity of all the possible hydrogen bonds. It takes into consideration the chemical environment of the donor/acceptor groups as well as other important factors, such as competition^[15] (as a function of total counts of donor and acceptor atoms), aromaticity and steric crowding.^[13b]

At the outset of any attempted “co-crystallisation reaction” it is not clear whether there will be any new phase. If there is a new phase it could be: a co-crystal; a salt; a salt or co-crystal solvate; a salt or co-crystal hydrate; or a hydrate or solvate of the reactants. In the work reported here the hydrogen bond propensity tool is applied to assess the likely outcome of attempted co-crystallisations.^[16] Using data in the CSD, the hydrogen bond propensity method can be equally applied to ionised or neutral species; all that is required is an appropriate description of the chemical groups as topological objects (see the Experimental Section for examples). Its application here can be interpreted as making an intelligent estimate of the success of supramolecular synthesis formation by extracting crystallographic knowledge stored in the CSD. We explore the predictability of salt, co-crystal or solvate formation using the hydrogen bond propensity tool. For this purpose we have chosen the anti-malarial drug pyrimethamine (**1**) as our model compound (Scheme 1).

Pyrimethamine is a challenging multifunctional molecule with numerous hydrogen bond forming groups. In addition, its low solubility in water makes the formation of molecular adducts an attractive proposition. In pyrimethamine the most basic site is N1 with a calculated pK_a value of 6.94. It is established that the pK_a of the reactants plays a very important role in the formation of a salt or co-crystal. Depending on the ΔpK_a (i.e., difference in pK_a of the most basic site on the base and most acidic site on the acid) either a salt or a co-crystal can form.^[2g,3a,18] Co-crystal formation is expected for $\Delta pK_a < 0$ and salt for $\Delta pK_a > 3$. A ΔpK_a value in the region 0–3 is less informative as to whether salt or co-crystal will form.^[3a,19]

Results and Discussion

Our first hydrogen bond propensity study was performed assuming neutral moieties and therefore the likelihood of co-crystal formation. The species (**a–j**) studied alongside **1** are listed in Scheme 1. We found that 7 out of 10 experiments resulted in salt formation. The ΔpK_a was calculated for the reactions **1a** to **1g**, which produced adducts. For **1a** to **1c**, ΔpK_a was found to be greater than 3 (Scheme 1), suggesting the likelihood of formation of salts, which was confirmed by determining their crystal structures from X-ray data (see later). But for adducts **1d** to **1g**, the ΔpK_a is between 0–3 in which case either a salt or a co-crystal might be expected. As we will show, however, experimentally **1d** to **1g** were also found to be salts. Jones and co-workers have previously reported the formation of various salts of pyrimethamine by



Reactants	Products and ratio	ΔpK_a^*
1+a	1a :CH ₃ OH (4:3:4)	5.71
1+b	1b :H ₂ O (2:2:1)	4.11
1+c	1c :CH ₃ OH (2:1:2)	5.21
1+d	1d (1:1)	2.52
1+e	1e (1:1)	2.46
1+f	1f :CH ₃ OH (2:1:6)	2.42
1+g	1g :CH ₃ OH (1:1:1)	2.39
1+h	Adduct formation was unsuccessful	
1+i		
1+j		

Scheme 1. ΔpK_a^* is the difference in pK_a of most basic atom on **1** and most acidic atom on the complementary acid.^[17] Throughout the study the same labels are used for: 1) neutral or ionic state of a molecule, and 2) reaction and reaction products. If a reaction product is solvated, then the presence of solvent is explicitly mentioned.

mechanochemistry.^[20] The difference between a salt or co-crystal product from these reactions is simply the migration of a proton from the acidic –COOH donor to a basic acceptor. Nevertheless, we subsequently carried out a second hydrogen bond propensity study with charged species. The results from both studies will be compared with the observed hydrogen bonding patterns found in the synthesised adducts.

To put the resulting reaction products into context it is useful to study the crystal structure of pure pyrimethamine

(CSD reference code: MUFMAB) reported by Muthiah and co-workers.^[21] Pyrimethamine molecules recognise each other by N–H···N dimeric hydrogen bonds utilising the most basic nitrogen at position 1 and the –NH₂ group attached to the carbon at 2 position from one side (motif 1: M1) and the less basic nitrogen at 3 position and –NH₂ group attached to carbon at position 4 on the other (motif 2: M2), forming tapes. The adjacent tapes further interact with each other utilising motif 3 (M3) forming sheets. Interaction between the tapes leads to the formation of a hydrogen-bonded system of three fused cyclic hydrogen-bonded ring motifs (M3M2M3) and is labelled as motif 4 (M4), as shown in Figure 1.

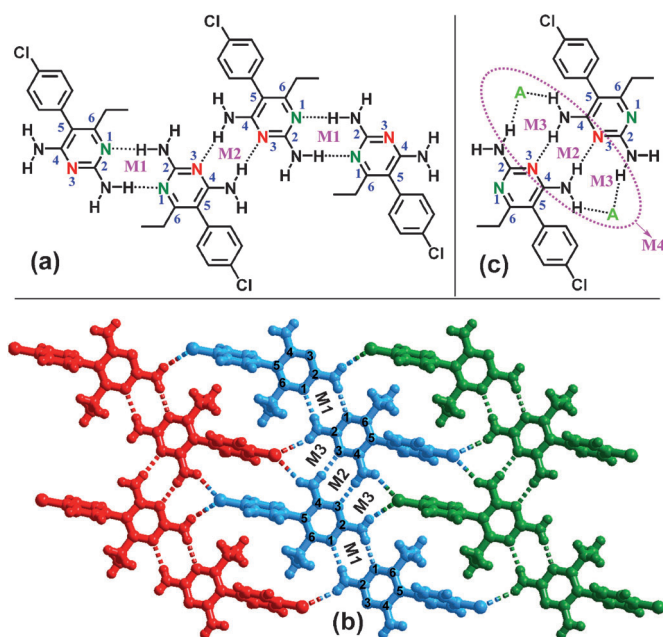
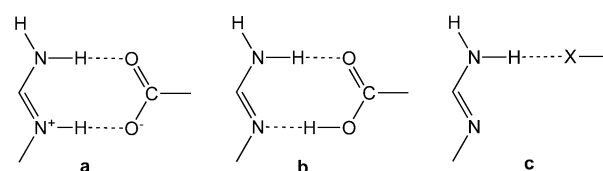


Figure 1. a) The molecules of **1** interact with each other by motifs 1 and 2 forming tapes. b) Adjacent tapes interact with each other by motif 3 forming sheets. c) Motif 4 (M4) is formed by the interaction between the adjacent tapes. Throughout this study the term M4 is used for all quadruple hydrogen-bonded motifs of three fused hydrogen-bonded motifs (M3M2M3), irrespective of the nature of acceptor A.

On crystallising **1** with **a–g**, the aminopyridine group of **1** can interact with acids either by aminopyridinium–carboxylate or aminopyridine–carboxylic acid heterosynthon, yielding salts and co-crystals, respectively. Conformers **h–j**, can interact with **1** by N–H···X hydrogen bonds (Scheme 2).

We attempted the crystallisation reaction of **1** with **a–j**. Adduct formation was successful between **1** and **a–g**, and unsuccessful for **1** and **h–j**. Hydrogen bond propensity calculations for co-crystallisation reactions were then compared with the outcome of our experiments and the results are summarised in Table 1. Our hypothesis was that the relative likelihood of individual hydrogen bonds to form between molecules of **1** or **a–j** only, that is, self-association, or involving both **1** and **a–j**, giving a molecular adduct, or indeed



Scheme 2. a), b) Heterosynthon between aminopyridine and carboxylic acid with and without proton transfer, respectively; c) aminopyridine–halogen bond.

with solvent, determines whether the desired adduct would be realised. This might be described as a competition between the hydrogen bond networks of pure reactants versus potential alternatives enabled through an additional counter molecule/ion or solvent. This first study was intended to predict the possible formation of co-crystals, and presents ranked propensity predictions for all unique hydrogen bonds that could form between neutral species with an indication of whether the interaction is between moieties of **1** only, or involves **1** and **a–j**. It is then possible to quickly visualise and compare the possible H bond outcomes. In our calculations we also considered the molecules of solvent (methanol) and water.

Predicted propensities for the successful reactions, **1a** to **1g**:

Table 1 reveals that in all adducts **1a** to **1g**, the four top-ranked predictions were between **1** and the acids suggesting the high likelihood of co-crystal formation. Moreover, it is interesting to note that since the functional groups involved in **1a** to **1g** are the same, in all the cases the first two predictions were between atom N7 as the donor and O9, O11 as the acceptors. The next two were between N8 and O9/O11. Since the propensity predictions between N7 and O9/O11 (propensity range of 0.90–0.92) are noticeably higher than between N8 and O9/O11 (propensity 0.83–0.86), the model suggests a higher probability of formation of a hydrogen bond between N7 and O9/O11. The next four bonds of highest propensity are predicted between solvent and acid or **1**, suggesting high likelihood of formation of solvates. Indeed 5 of these 7 reactions have yielded solvates (**1a**, **1c**, **1f**, **1g** crystallised as methanol solvates and **1–b** as hydrate). Since we have used methanol as the solvent in all co-crystallisations there is a greater chance of formation of a methanol solvate than a hydrate. The source of the water (in hydrated adduct, such as **1b**) might be atmospheric or small amounts present in the methanol.

Predicted propensities for the unsuccessful reactions, **1h** to **1j**:

Encouraged by the success of the propensity model in predicting co-crystal formation with **1**, we aimed to check the ability of the propensity model to discriminate against less suitable conformers for **1**. We planned crystallisation of **1** with **h–j**. Since in **1h** to **1j**, only single hydrogen bonds (N–H···X) are available as alternatives to the aminopyridine and carboxylic acid homodimers of **1** and acids, respectively, difficulties in synthesising possible adducts were to be ex-

Table 1. Predicted and experimental results of crystallisation of **1** and **a–j** as neutral species in the presence of methanol (solvent used for co-crystallisations) and water.

Reaction	Numbering scheme of model taken	Bonds of highest propensity ^[a]			Type of interaction ^[b]	Predicted result	Experimental result
		donor	acceptor	propensity			
1a		N7	O9	0.92	A	co-crystal formation	salt formed (methanol solvate)
		N7	O11	0.92	A		
		N8	O11	0.86	A		
		N8	O9	0.86	A		
		O14	O11	0.81	B		
		O14	O9	0.81	B		
1b		N7	O9	0.91	A	co-crystal formation	salt formed (hydrate)
		N7	O11	0.91	A		
		N8	O11	0.85	A		
		N8	O9	0.85	A		
		O14	O9	0.79	B		
		O14	O11	0.79	B		
1c		N7	O9	0.91	A	co-crystal formation	salt formed (methanol solvate)
		N7	O11	0.91	A		
		N8	O9	0.86	A		
		N8	O11	0.86	A		
		O14	O9	0.80	B		
		O14	O11	0.80	B		
1d		N7	O9	0.90	A	co-crystal formation	salt formed (non-solvated)
		N7	O11	0.90	A		
		N8	O9	0.83	A		
		N8	O11	0.83	A		
		N7	O14	0.77	B		
		O14	O11	0.77	B		
1e		N7	O9	0.90	A	co-crystal formation	salt formed (non-solvated)
		N7	O11	0.90	A		
		N8	O9	0.83	A		
		N8	O11	0.83	A		
		N7	O14	0.77	B		
		O14	O9	0.77	B		
1f		N7	O9	0.90	A	co-crystal formation	salt formed (methanol solvate)
		N7	O11	0.90	A		
		N8	O9	0.83	A		
		N8	O11	0.83	A		
		O14	O11	0.77	B		
		O14	O9	0.77	B		

pected. In **1h** to **1j**, the bonds of highest propensity (first two for **1h**, **1j** and first three for **1i**) are between **1** and methanol or water. The next bond (3rd for **1h**, **1j** and 4th for **1i**) is for the self-association of molecules of **1**. Since the propensity of bonds for co-crystal formation (14th bond for **1h**,

1i; propensity 0.41, 0.33, respectively) and 11th for **1j** (propensity 0.41; see Tables S8–S10 in the Supporting Information for full propensity calculations for **1h** to **1j**) is significantly lower compared to those of highest propensity (propensity 0.79–0.87), we can conclude that the propensity

Table 1. (Continued)

Reaction	Numbering scheme of model taken	Bonds of highest propensity ^[a]			Type of interaction ^[b]	Predicted result	Experimental result
		donor	acceptor	propensity			
1g		N7	O9	0.90	A	co-crystal formation	salt formed (methanol solvate)
		N7	O11	0.90	A		
		N8	O11	0.83	A		
		N8	O9	0.83	A		
		O14	O11	0.77	B		
		O14	O9	0.77	B		
		N7	O14	0.77	B		
1h		N7	O13	0.87	B	self-association ^[c]	co-crystal did not form
		N7	O14	0.87	B		
		N7	N1	0.76	C		
		N8	O13	0.76	B		
		N8	O14	0.76	B		
		N7	N3	0.65	C		
		O14	O13	0.63	B		
1i		N7	O13	0.79	B	self-association ^[c]	co-crystal did not form
		N7	O14	0.79	B		
		N8	O13	0.67	B		
		N7	N1	0.67	C		
		N8	O14	0.67	B		
		O14	O13	0.56	B		
		O14	O14	0.55	B		
1j		N7	O14	0.84	B	self-association ^[c]	co-crystal did not form
		N7	O13	0.83	B		
		N7	N1	0.73	C		
		N8	O14	0.72	B		
		N8	O13	0.71	B		
		O14	O14	0.63	B		
		O14	O13	0.62	B		

[a] A full list of propensity predictions is given in Tables S1–S10 in the Supporting Information. [b] **A** represents interaction between **1** and **a–j**, **B** represents interaction of **1**, **a–j** or solvent with solvent, and **C** represents self-assembly of molecules of **1** or **a–j**. [c] Self-association of molecules predicted: calculations also indicate the possibility for **1** crystallizing as solvate.

model suggests little chance of **1** interacting with **h–j** to form a co-crystal (Table 1). It is also possible that a co-crystal might form even without interaction between the two components; the propensity calculations are, of course, limited in their use for predicting adducts formed in this way. The bonds of the highest propensity calculated between **1** and solvent, strongly suggests the possible formation of solvate of **1**. Reactants of **1h** to **1j** did not interact with each other to form co-crystals, as shown by the comparison of PXRD plots (Table S18 in the Supporting Information). The PXRD suggested that the reactants simply crystallised out separately without the formation of solvate. An attempt to obtain a methanol solvate of pyrimethamine by crystallising it from methanol failed as indicated by the comparison of the PXRD plot of the material so obtained with that of pure pyrimethamine. However, a new material was obtained by grinding pyrimethamine in the presence of a small amount

of methanol. The material was subsequently characterised as a methanol solvate of **1** by single-crystal XRD (Table S20 in the Supporting Information).

Hydrogen-bond propensity calculations for adducts 1a to 1g based on charged species: It was encouraging to note that the propensity calculations for co-crystal formation between the neutral molecules of **1** and acids (**a–g**) predicted the formation of co-crystals. Subsequent experiments, however, revealed the products **1a** to **1g** to be salts as a result of the transfer of a proton from the acid to the most basic nitrogen (N1) of **1**, creating a short, strong hydrogen bond of length in the range 1.78–1.90 Å in **1a** to **1g**. We, therefore, repeated the propensity calculations for **1a** to **1g**, representing the molecules using charged functional groups, as appropriate, consistent with the observed crystal structures. On the basis of this evidence, for routine employment of the method as

a screening tool, it would be advisable to investigate models for both neutral and charged adducts. As mentioned previously, a priori anticipation of product as a salt or co-crystal is difficult, especially for co-crystallisations with ΔpK_a in the range 0–3.

Seven new propensity models were trained by using modified functional groups consistent with the ions of the observed crystal structures (Scheme 2, a). We again considered the presence of methanol and water. Our view was that our initial expectations would be confirmed, because by adding opposite charges on **1** and species a–g the chances for interaction should increase. The calculations supported our assumption. On comparing the values of the bonds of highest propensity in Table 2 with Table 1, it is clear that the computed propensity values involving charged species increased. In Table 2, we have given the first seven predictions (a full list is given in Tables S11–S17 in the Supporting Information). Analysis of these first seven predictions revealed that in **1a** to **1g** the bonds of highest propensity are between cationic **1** and acid anions, and hence our model successfully predicts the formation of salts between **1** and a–g.

Crystal structures of the observed reaction products: Formation of adduct **1a** to **1g** was confirmed by single-crystal XRD. The materials were further characterised by using thermal techniques, such as thermogravimetric analysis (TGA) and differential scanning calorimetry (DSC; Table S19 in the Supporting Information)

Salt between pyrimethamine and oxalic acid, 1a: Salt **1a** was obtained as a methanol solvate on crystallising **1** and **a** from a 1:1 mixture in methanol. In the salt, the ions of **1** and **a** recognise each other and form molecular tapes (Figure 2). There are two types of ions of pyrimethaminium (labelled **A** and **B**) and of deprotonated oxalic acid (labelled **C** (monodeprotonated) and **D** (doubly deprotonated), respectively). In the tape network of **1a**, the most basic protonated nitrogen (N1) and the $-\text{NH}_2$ group at adjacent carbon (C2) of both **A** and **B** type of cations of pyrimethaminium recognise the complementary carboxylate group on anions **C** and **D**, respectively, by utilising hydrogen-bonded motif 5 (M5). **A** and **B** recognise each other by N–H...N dimeric hydrogen-bonded motif 6 (M6) with H...N distance of 2.12 and 2.51 Å by using nitrogen at the 3 position and $-\text{NH}_2$ group attached to carbon at 4 and 2 position of **A** and **B**, respectively. It is noteworthy that motif 6 was not observed in the structure of **1**. In addition in the tape network the O–H...O[−] interactions (H...O[−] distance 1.73) were also observed between the **C** and **D**. The oxygen atom of methanol interacts with pyrimethaminium in the same layer by N–H...O hydrogen bonds (H...O distances 2.09, 2.11, 2.12 Å).

Salt between pyrimethamine and malonic acid, 1b: In **1b**, the ions of **1** and **b** recognise each other to form molecular tapes (Figure 3). In the salt there are two types of molecular ions of pyrimethaminium (labelled **A** and **B**) and deprotonated malonic acid (labelled **C** and **D**; both monodeprotonat-

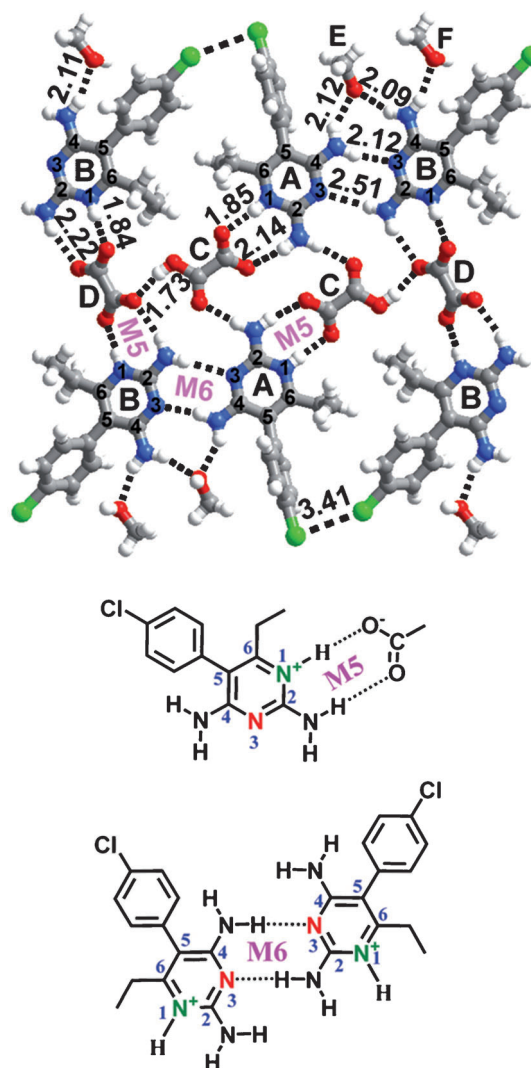


Figure 2. Tape network observed in **1a**. M5 and M6 are the motifs 5 and 6, respectively.

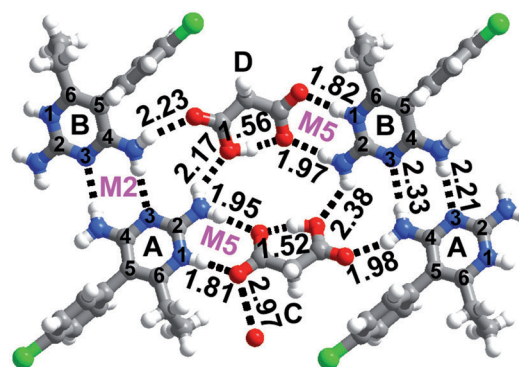


Figure 3. Recognition pattern as observed in **1b**.

ed). As observed in **1a**, **A** and **B** recognise the complementary carboxylate group of **C** and **D**, respectively, by motif 5 (M5) with H...O[−] distances 1.81, 1.82 and 1.95, 1.97 Å. **A** and **B** recognise each other by motif 2 (M2) with H...N distance of 2.21 and 2.33 Å. Whereas the $-\text{OH}$ of the carboxyl-

nium cations recognise each other by motif 2 as also observed in the crystal structure of **1**, **1b** and **1c**. Whereas the -OH group of carboxylic acid functional group of **e** is found to be involved in a $\text{O-H}\cdots\text{O}^-$ hydrogen bond ($\text{H}\cdots\text{O}^-$ distance 1.61 Å) with another molecule of **e** in the same layer, the carbonyl of carboxylic acid functional group forms $\text{N-H}\cdots\text{O}$ hydrogen bonds ($\text{H}\cdots\text{O}$ distance of 2.16, 2.22 Å) with the -NH_2 groups of molecules of **1** in adjacent layers, forming motif 3. Interaction of a tape (shown in red in the Figure 6b) with the acid molecules in the layer above and below (shown in blue and green in the Figure 6b) leads to the formation of motif 4 (M4).

Salt between pyrimethamine and suberic acid, 1f: In the 2:1 adduct observed between **1** and **f**, the molecules of suberic acid are doubly deprotonated. The pyrimethaminium cations interact with each other by motif 2 forming dimers (Figure 7). Further the -NH_2 group at C2 and C4 of **1**, inter-

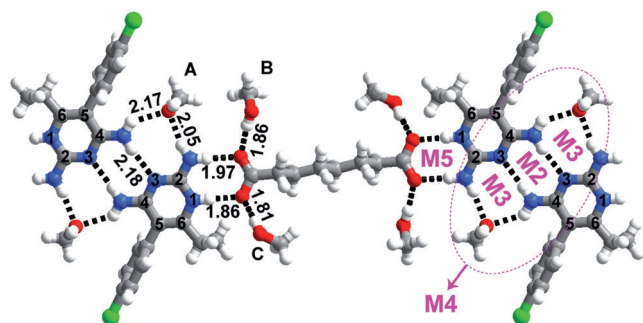


Figure 7. Recognition pattern observed in **1f**.

acted with an oxygen atom of the methanol molecules (labelled **A**) by motif 3 forming tetramer. It also leads to the formation of motif 4 (M4), as also observed in the crystal structure of **1** and **1e**. The deprotonated acid molecules connect the adjacent tetramers by motif 5. In addition, the methanol molecules (labelled **B** and **C**) interact with the carboxylate oxygen of the acid by $\text{O-H}\cdots\text{O}^-$ hydrogen bonds ($\text{H}\cdots\text{O}^-$ distances 1.81 and 1.86 Å).

Salt between pyrimethamine and azelaic acid, 1g: In **1g**, ions of **1** recognise the carboxylate group of the deprotonated aliphatic acid by motif 5 (Figure 8a). The pyrimethaminium cations recognised each other by motif 2, as also observed in the crystal structure of **1** and **1b**, **1c**, **1e** and **1f**. While the carbonyl group of carboxylic acid functional group of azelaic acid is involved in $\text{N-H}\cdots\text{O}$ hydrogen bonds, forming motif 3 ($\text{H}\cdots\text{O}$ distances 2.21, 2.31 Å), the hydroxyl group of the carboxylic acid functional group recognises adjacent layers by $\text{O-H}\cdots\text{O}^-$ hydrogen bonds ($\text{H}\cdots\text{O}^-$ distance 1.74 Å), as shown in Figure 8b. In **1g** motif 4 (M4) is also observed, as in case of **1**, **1e** and **1f**.

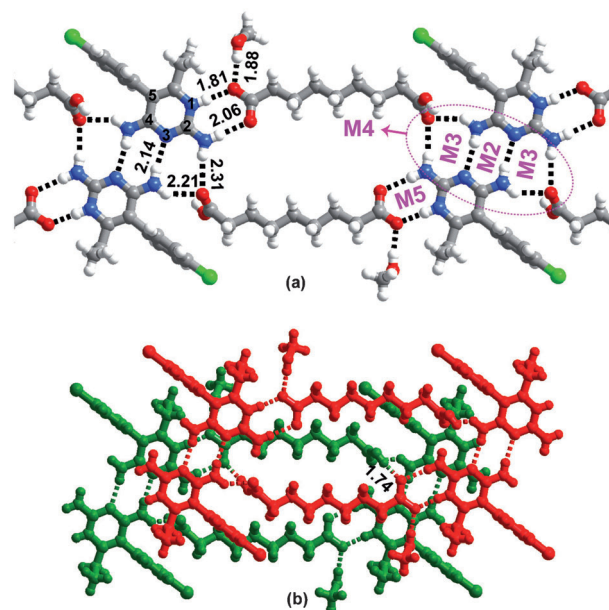


Figure 8. a) Tape network observed in **1g**. b) interactions observed between the adjacent tapes.

Conclusions

Crystallisation reactions **1a** to **1j** were carried out between pyrimethamine and various counter molecules (**a-j**), of which **1a** to **1g** were successful in forming adducts. Hydrogen bond propensity calculations were performed along with the experimental work to validate the use of this tool in predicting the formation of salts/co-crystals. Calculations correctly predicted the formation and non-formation of adducts in **1a** to **1g** and **1h** to **1j**, respectively. All seven successful adducts formed were found to be salts. Predictions were made both assuming neutral species forming co-crystals and charged species forming salts, with comparable results.

Though propensity calculations correctly predicted the outcome of crystallisation reactions **1a** to **1j**, to verify the general applicability of these calculations in predicting the formation of adducts, comparison of predicted and experimental results with molecules containing a wider range of functional groups is required. This work is currently underway, with encouraging preliminary results. It is worth noting that as the propensity calculations make use of the CSD, the predictions will continue to grow in accuracy with the addition of more relevant crystallographic data.

Experimental Section

General: All the chemicals used in this study were obtained from Aldrich and were used without further purification. The solvents employed for the crystallisations were of spectroscopy grade of highest available purity. All the crystallisation reactions were completed by dissolving **1** and **a-j** in 1:1 ratio in a CH_3OH solvent and slow evaporation of the obtained solution. Single crystals of the salts **1a** to **1g** were obtained over a period of 48 h. In a typical preparation, **1** (0.1244 g; 0.5 mmol) and adipic acid

(0.0731 g; 0.5 mmol) were dissolved in CH₃OH (15 mL) by being gently warmed on a hot plate. The resultant solution was kept for evaporation at ambient conditions by protecting the conical flask from external mechanical disturbances. Within 48 h, colourless and good-quality crystals of **1d**, were obtained that were suitable for studies by single crystal X-ray diffraction methods. As reactions **1h** to **1j** were unable to give adducts from solution, we also tried to form adducts by liquid-assisted-grinding,^[23] but LAG also failed to yield adducts.

A methanol solvate of pyrimethamine was obtained by LAG and was structurally characterised by single crystal XRD. The crystals of methanol solvate of **1** were obtained by seeding methanol solution of **1** with seeds obtained by LAG. All the LAG experiments were carried by grinding the reactants (0.5 mmol) at 30 Hz for 30 min in the presence of methanol (30 μL).

Crystal structure determination of 1a to 1g: Good quality single crystals of **1a** to **1g** were chosen by viewing under microscope and glued to a glass fibre and mounted on a goniometer of a Bruker single-crystal X-ray diffractometer equipped with APEX CCD detector. The data collections were smooth in all the cases without any complications and all the crystals were found to be stable throughout data collection period. The intensity data were processed by using Bruker suite of programs,^[24] SAINT, followed by absorption correction by SADABS.^[24] The structures were solved using SHELXS and refined by least-square methods with SHELXL.^[24] All the non-hydrogen atoms were refined by anisotropic methods and the hydrogen atoms were either refined or placed in the calculated positions. All the structural refinements converged to good *R* factors (Table 3) and the intermolecular interactions were computed by using PLATON software,^[25] and are given in Table 4. The packing diagrams were generated by using Diamond, version 3.1e.^[26]

CCDC 846669–846675 and 859637 contain the supplementary crystallographic data for this paper. These data can be obtained free of charge from The Cambridge Crystallographic Data Centre via www.ccdc.cam.ac.uk/data_request/cif.

Hydrogen bond propensity prediction: Predictive models were prepared by using a development version of Mercury 3.0 (pre-release)^[16] and the CSD v.5.32 (November, 2010). The neutral models used functional groups as displayed in Scheme 3 a–h and the charged models used groups as shown in Scheme 3 i–o. In total ten neutral models and seven charged models were prepared for molecule **1** and co-formers **a–j** and **a–g**, respectively. For each model roughly 1000 CSD structures were used as the data source to fit the model (the least being 955 for model **1h** and the most being 1407 for model **1b**; see Table S21 in the Supporting Information for details). In these calculations functional groups of water and methanol were also considered. Acceptance criteria for the propensity models were that each functional group is represented in >250 structures. The minimum predictivity observed was >78%.

Acknowledgements

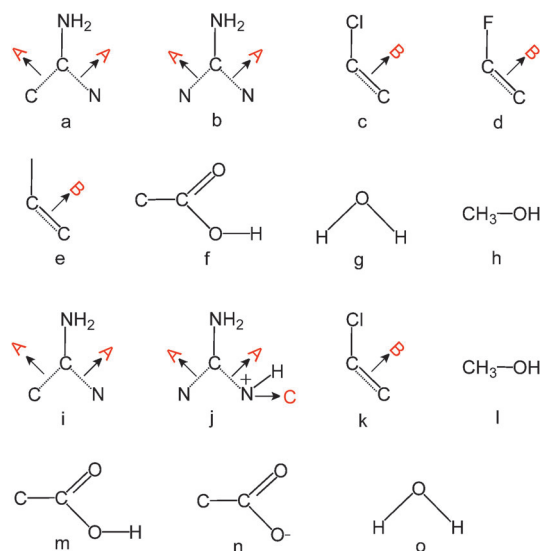
We thank the Pfizer Institute for Pharmaceutical Materials Science for funding (Fellowship for A.D.). We acknowledge Dr. Neil Feeder (Pfizer Global R&D) and Dr. Colin Groom (CCDC) for helpful discussions. The CCDC is thanked for providing a new version of the Mercury software for the propensity calculations; Dr. James Chisholm for discussions regarding the use of these propensity calculations and Dr. John E. Davies for collecting single-crystal X-ray data for the reported adducts.

Table 3. Crystallographic data for the adducts **1a** to **1g**.

	1a	1b	1c	1d	1e	1f	1g
formula	2(C ₁₂ H ₁₄ N ₄ Cl ₁): C ₂ H ₄ O ₄ : 0.5(C ₂ O ₄): 2(CH ₄ O)	2(C ₁₂ H ₁₄ N ₄ Cl ₁): 2(C ₃ H ₃ O ₄): H ₂ O	2(C ₁₂ H ₁₄ N ₄ Cl ₁): C ₂ O ₄ : 2(CH ₄ O)	C ₁₂ H ₁₄ N ₄ Cl ₁ : C ₆ H ₉ O ₄	C ₁₂ H ₁₄ N ₄ Cl ₁ : C ₇ H ₁₁ O ₄	C ₁₂ H ₁₄ N ₄ Cl ₁ : 0.5(C ₈ H ₁₂ O ₄): 3(CH ₄ O)	C ₁₂ H ₁₄ N ₄ Cl ₁ : C ₉ H ₁₅ O ₄ : CH ₄ O
<i>M_r</i>	696.57	723.57	675.57	394.85	408.88	431.94	468.97
crystal habit	blocks	blocks	needles	rod-shaped	rectangular blocks	rectangular blocks	rods
crystal colour	colourless	colourless	colourless	colourless	colourless	colourless	colourless
crystal system	triclinic	triclinic	monoclinic	triclinic	triclinic	monoclinic	triclinic
space group	<i>P</i> $\bar{1}$	<i>P</i> $\bar{1}$	<i>P</i> 2 ₁ / <i>c</i>	<i>P</i> $\bar{1}$	<i>P</i> $\bar{1}$	<i>P</i> 2 ₁ / <i>c</i>	<i>P</i> $\bar{1}$
<i>a</i> [Å]	10.545(2)	9.377(2)	13.866 (2)	8.080(1)	6.925(2)	9.346(1)	6.604 (2)
<i>b</i> [Å]	12.183(2)	11.746(2)	7.0299 (1)	11.174(2)	11.188(3)	15.398(2)	13.278(4)
<i>c</i> [Å]	14.248(3)	16.110(3)	36.562(5)	12.100(2)	13.429(3)	18.060(2)	15.205(5)
α [°]	74.55(1)	72.40(1)	90.00	88.65(1)	92.83 (1)	90.00	114.56 (2)
β [°]	80.24(1)	85.34(1)	109.03 (1)	70.51(1)	92.21(1)	113.70(1)	92.63 (2)
γ [°]	69.57(1)	78.11(1)	90.00	72.03(1)	97.63 (1)	90.00	95.44 (2)
<i>V</i> [Å ³]	1647.23(5)	1654.77(5)	3369.22(8)	975.79(3)	1028.77(5)	2379.65(5)	1201.76(6)
<i>Z</i>	2	2	4	2	2	4	2
ρ_{calcd} [g cm ⁻³]	1.404	1.452	1.332	1.344	1.320	1.206	1.296
<i>T</i> [K]	180(2)	180(2)	180(2)	180(2)	180(2)	180(2)	180(2)
λ (MoK α)	0.71073	0.71073	0.71073	0.71073	0.71073	0.71073	0.71073
μ [mm ⁻¹]	0.259	0.263	0.246	0.227	0.218	0.195	0.198
2 θ range [°]	64.12	55.78	50.02	58.26	55.74	54.96	55.66
limiting indices	-15 ≤ <i>h</i> ≤ 15 -18 ≤ <i>k</i> ≤ 18 -17 ≤ <i>l</i> ≤ 21	-12 ≤ <i>h</i> ≤ 12 -15 ≤ <i>k</i> ≤ 15 -21 ≤ <i>l</i> ≤ 21	-16 ≤ <i>h</i> ≤ 16 -8 ≤ <i>k</i> ≤ 8 -43 ≤ <i>l</i> ≤ 43	-10 ≤ <i>h</i> ≤ 11 -15 ≤ <i>k</i> ≤ 15 -16 ≤ <i>l</i> ≤ 16	-9 ≤ <i>h</i> ≤ 9 -14 ≤ <i>k</i> ≤ 14 -17 ≤ <i>l</i> ≤ 17	-12 ≤ <i>h</i> ≤ 12 -19 ≤ <i>k</i> ≤ 19 -23 ≤ <i>l</i> ≤ 23	-8 ≤ <i>h</i> ≤ 8 -17 ≤ <i>k</i> ≤ 17 -18 ≤ <i>l</i> ≤ 19
<i>F</i> (000)	730	756	1416	416	432	924	500
reflns measured	31 494	27 346	30 778	19 164	15 131	26 096	11 961
unique reflns	11 422	7868	5920	5238	4878	5437	5629
reflns used	6180	5577	4750	3879	3741	4582	2843
parameters	442	444	419	248	257	266	296
GOF on <i>F</i> ²	0.955	1.023	1.024	1.066	1.034	1.064	0.912
<i>R</i> ₁ [<i>I</i> > 2 σ (<i>I</i>)]	0.0599	0.0538	0.0443	0.0494	0.0569	0.0480	0.0499
<i>wR</i> ₂	0.1191	0.1300	0.1086	0.1221	0.1504	0.1325	0.1012
largest diff. peak/hole [e ⁻ Å ⁻³]	0.065/−0.598	1.063/−0.505	0.337/−0.475	0.310/−0.328	0.498/−0.523	0.425/−0.416	0.193/−0.259

Table 4. Bond length and angles of the hydrogen bonds observed in adducts **1a** to **1g**.

Hydrogen bond	1a			1b			1c			1d			1e			1f			1g		
D-H...A																					
N-H...N	2.12	2.98	165	2.21	3.08	169	2.10	2.97	171				2.11	2.97	166	2.18	3.06	172	2.14	3.02	172
	2.51	3.33	155	2.33	3.18	162	2.22	3.10	175												
	2.04	2.91	169	1.98	2.83	160	2.06	2.89	156	2.04	2.91	168	2.16	3.02	166	2.05	2.91	168	2.21	2.94	140
N-H...O	2.09	2.93	160	2.17	2.83	132	2.20	2.91	137	2.22	2.93	137	2.22	2.91	135	2.17	2.84	133	2.31	3.17	166
	2.11	2.93	155	2.23	3.04	152															
	2.12	2.88	145	2.38	2.99	127															
	2.14	2.94	152	1.95	2.82	170	1.92	2.80	176	2.04	2.91	167	1.95	2.83	175	1.97	2.80	157	2.06	2.93	177
N-H...O ⁻	2.22	3.06	160	1.97	2.85	175	1.93	2.80	172	2.21	2.88	133									
							2.09	2.85	145												
N ⁺ -H...O ⁻	1.83	2.71	173	1.81	2.71	171	1.81	2.69	178	1.80	2.68	177	1.78	2.65	169	1.86	2.72	174	1.81	2.68	170
	1.85	2.73	178	1.82	2.73	172	1.90	2.78	176												
O-H...O							1.83	2.73	169							1.91	2.70	168			
	1.74	2.64	170	1.52	2.47	162	1.87	2.71	169	1.68	2.55	167	1.61	2.49	172	1.81	2.66	176	1.74	2.59	174
O-H...O ⁻	1.92	2.75	168	1.56	2.48	158										1.86	2.72	174	1.88	2.77	176
	1.93	2.77	169																		
C-H...O	2.57	3.34	139	2.28	3.20	160				2.53	3.49	161									
C-H...O ⁻				2.56	3.43	152	2.52	3.39	152	2.52	3.39	151									
C-H...Cl							2.79	3.48	128												



Scheme 3. Hydrogen bond definitions used for predicting: a)–h) various co-crystals, and i)–o) salts of pyrimethamine. A=cyclic bonds with variable bond type (single, double, aromatic, delocalised); B=aromatic; C=number of bonded atoms is 3.

- [1] a) S. G. Fleischman, S. S. Kuduva, J. A. McMahon, B. Moulton, R. D. B. Walsh, N. Rodríguez-Hornedo, M. J. Zaworotko, *Cryst. Growth Des.* **2003**, *3*, 909; b) P. Vishweshwar, J. A. McMahon, M. L. Peterson, M. B. Hickey, T. R. Shattock, M. J. Zaworotko, *Chem. Commun.* **2005**, 4601; c) S. N. Black, E. A. Collier, R. J. Davey, R. J. Roberts, *J. Pharm. Sci.* **2007**, *96*, 1053; d) K. K. Arora, N. G. Tayade, R. Suryanarayanan, *Mol. Pharm.* **2011**, *8*, 982; e) T. Frišćić, W. Jones, *J. Pharm. Pharmacol.* **2010**, *62*, 1547; f) J. R. G. Sander, D.-K. Bučar, R. F. Henry, G. G. Z. Zhang, L. R. MacGillivray, *Angew. Chem.* **2010**, *122*, 7442; *Angew. Chem. Int. Ed.* **2010**, *49*, 7284; g) J. A. Foster, M.-O. M. Piepenbrock, G. O. Lloyd, N. Clarke, J. A. K. Howard, J. W. Steed, *Nat. Chem.* **2010**, *2*, 1037.
- [2] a) J. F. Remenar, S. L. Morissette, M. L. Peterson, B. Moulton, J. M. MacPhee, H. R. Guzmán, Ö. Almarsson, *J. Am. Chem. Soc.* **2003**, *125*, 8456; b) P. M. Bhatt, N. V. Ravindra, R. Banerjee, G. R. Desira-

ju, *Chem. Commun.* **2005**, 1073; c) J. Galcera, E. Molins, *Cryst. Growth Des.* **2009**, *9*, 327; d) R. Banerjee, P. M. Bhatt, N. V. Ravindra, G. R. Desiraju, *Cryst. Growth Des.* **2005**, *5*, 2299; e) D. J. Good, N. Rodríguez-Hornedo, *Cryst. Growth Des.* **2010**, *10*, 1028; f) S. J. Bethune, N. Huang, A. Jayasankar, N. Rodríguez-Hornedo, *Cryst. Growth Des.* **2009**, *9*, 3976; g) C. L. Cooke, R. J. Davey, *Cryst. Growth Des.* **2008**, *8*, 3483; h) C. B. Aakeröy, S. Forbes, J. Desper, *J. Am. Chem. Soc.* **2009**, *131*, 17048; i) R. Thakuria, A. Nangia, *CrystEngComm* **2011**, *13*, 1759; j) S. Ghosh, P. P. Bag, C. M. Reddy, *Cryst. Growth Des.* **2011**, *11*, 3489.

- [3] a) M. L. Cheney, N. Shan, E. R. Healey, M. Hanna, L. Wojtas, M. J. Zaworotko, V. Sava, S. J. Song, J. R. Sanchez-Ramos, *Cryst. Growth Des.* **2010**, *10*, 394; b) M. B. Hickey, M. L. Peterson, L. A. Scoppettuolo, S. L. Morissette, A. Vetter, H. Guzmán, J. F. Remenar, Z. Zhang, M. D. Tawa, S. Haley, M. J. Zaworotko, O. Almarsson, *Eur. J. Pharm. Biopharm.* **2007**, *67*, 112; c) D. P. McNamara, S. L. Childs, J. Giordano, A. Iarriccio, J. Cassidy, M. S. Shet, R. Mannion, E. O'Donnell, A. Park, *Pharm. Res.* **2006**, *23*, 1888.
- [4] a) R. D. B. Walsh, M. W. Bradner, S. Fleischman, L. A. Morales, B. Moulton, N. Rodríguez-Hornedo, M. J. Zaworotko, *Chem. Commun.* **2003**, 186; b) D. Braga, E. Dichiarante, G. Palladino, F. Grepioni, M. R. Chierotti, R. Gobetto, L. Pellegrino, *CrystEngComm* **2010**, *12*, 3534.
- [5] a) A. V. Trask, W. D. S. Motherwell, W. Jones, *Cryst. Growth Des.* **2005**, *5*, 1013; b) A. V. Trask, W. D. S. Motherwell, W. Jones, *Int. J. Pharm.* **2006**, *320*, 114.
- [6] a) S. Karki, T. Frišćić, L. Fabian, P. R. Laity, G. M. Day, W. Jones, *Adv. Mater.* **2009**, *21*, 3905; b) C. M. Reddy, K. A. Padmanabhan, G. R. Desiraju, *Cryst. Growth Des.* **2006**, *6*, 2720.
- [7] a) S. Karki, T. Frišćić, L. Fábán, W. Jones, *CrystEngComm* **2010**, *12*, 4038; b) S. R. Perumalla, E. Suresh, V. R. Pedireddi, *Angew. Chem.* **2005**, *117*, 7930; *Angew. Chem. Int. Ed.* **2005**, *44*, 7752.
- [8] a) D. Musumeci, C. A. Hunter, R. Prohens, S. Scuderi, J. F. McCabe, *Chem. Sci.* **2011**, *2*, 883; b) C. A. Hunter, *Angew. Chem.* **2004**, *116*, 5424; *Angew. Chem. Int. Ed.* **2004**, *43*, 5310; c) C. B. Aakeröy, J. Desper, M. M. Smith, *Chem. Commun.* **2007**, 3936; d) T. S. Thakur, G. R. Desiraju, *Cryst. Growth Des.* **2008**, *8*, 4031.
- [9] N. Issa, P. G. Karamertzanis, G. W. A. Welch, S. L. Price, *Cryst. Growth Des.* **2009**, *9*, 442.
- [10] a) L. Fábán, *Cryst. Growth Des.* **2009**, *9*, 1436; b) J. Fayos, *Cryst. Growth Des.* **2009**, *9*, 3142.
- [11] a) G. R. Desiraju, *Angew. Chem.* **1995**, *107*, 2541; *Angew. Chem. Int. Ed. Engl.* **1995**, *34*, 2311; b) S. Varughese, Y. Azim, G. R. Desiraju, *J. Pharm. Sci.* **2010**, *99*, 3743; c) R. Banerjee, B. K. Saha, G. R. Desiraju, *CrystEngComm* **2006**, *8*, 680; d) B. Sarma, N. K. Nath, B. R.

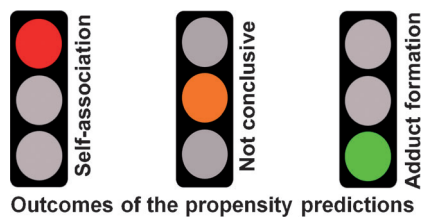
- Bhogala, A. Nangia, *Cryst. Growth Des.* **2009**, *9*, 1546; e) T. R. Shat-tock, K. K. Arora, P. Vishweshwar, M. J. Zaworotko, *Cryst. Growth Des.* **2008**, *8*, 4533.
- [12] P. M. Bhatt, Y. Azim, T. S. Thakur, G. R. Desiraju, *Cryst. Growth Des.* **2009**, *9*, 951.
- [13] a) J. Christolm, E. Pidcock, J. van de Streek, L. Infantes, S. Motherwell, F. H. Allen, *CrystEngComm* **2006**, *8*, 11; b) P. A. Wood, P. T. A. Galek, *CrystEngComm* **2010**, *12*, 2485.
- [14] a) P. T. A. Galek, L. Fabian, W. D. S. Motherwell, F. H. Allen, N. Feeder, *Acta Crystallogr. Sect. B* **2007**, *63*, 768; b) P. T. A. Galek, F. H. Allen, L. Fabian, N. Feeder, *CrystEngComm* **2009**, *11*, 2634; c) P. T. A. Galek, L. Fabian, F. H. Allen, *CrystEngComm* **2010**, *12*, 2091; d) P. T. A. Galek, L. Fabian, F. H. Allen, *Acta Crystallogr. Sect. B* **2010**, *66*, 237; e) P. T. A. Galek, E. Pidcock, P. A. Wood, I. J. Bruno, C. R. Groom, *CrystEngComm* **2012**, *14*, 2391.
- [15] L. Infantes, W. D. S. Motherwell, *Z. Kristallogr.* **2005**, *220*, 333.
- [16] Propensity calculations were carried out with a newer version of mercury software (mercury 2.4.1 cfc), which is under development by CCDC. For these calculations conquest version 1.13 was used as database.
- [17] The pK_a value of pyrimethamine was calculated by using sparc online calculator <http://sparc.chem.uga.edu/sparc/>. The pK_a values of acids were obtained from: pK_a Data Compiled by R. Williams.
- [18] a) B. R. Bhogala, S. Basavoju, A. Nangia, *CrystEngComm* **2005**, *7*, 551; b) A. Delori, E. Suresh, V. R. Pedireddi, *Chem. Eur. J.* **2008**, *14*, 6967.
- [19] a) M. L. Cheney, D. R. Weyna, N. Shan, M. Hanna, L. Wojtas, M. J. Zaworotko, *Cryst. Growth Des.* **2010**, *10*, 4401; b) C. B. Aakeröy, A. Rajbanshi, Z. J. Li, J. Desper, *CrystEngComm* **2010**, *12*, 4231; c) C. B. Aakeröy, M. E. Fasulo, J. Desper, *Mol. Pharm.* **2007**, *4*, 317.
- [20] a) A. V. Trask, D. A. Haynes, W. D. S. Motherwell, W. Jones, *Chem. Commun.* **2006**, 51; b) V. Sethuraman, N. Stanley, P. T. Muthiah, W. S. Sheldrick, M. Winter, P. Luger, M. Weber, *Cryst. Growth Des.* **2003**, *3*, 823; c) N. Stanley, V. Sethuraman, P. T. Muthiah, P. Luger, M. Weber, *Cryst. Growth Des.* **2002**, *2*, 631.
- [21] V. Sethuraman, P. T. Muthiah, *Acta Crystallogr. Sect. E* **2002**, *58*, o817.
- [22] P. Devi, P. T. Muthiah, T. N. Guru Row, V. Thiruvengadam, *Acta Crystallogr. Sect. E* **2007**, *63*, o4065.
- [23] N. Shan, F. Toda, W. Jones, *Chem. Commun.* **2002**, 2372.
- [24] a) Siemens, SMART System, Siemens Analytical X-ray Instruments Inc., Madison, WI (USA), **1995**; b) G. M. Sheldrick, Siemens Area Detector Absorption Correction Program (SADABS), University of Göttingen, Göttingen, Germany, **1994**; c) G. M. Sheldrick, SHELXTL-PLUS program for crystal structure solution and refinement, University of Göttingen, Göttingen, Germany.
- [25] A. L. Spek, PLATON, molecular geometry program, University of Utrecht, The Netherlands, **1995**.
- [26] Diamond-Crystal and Molecular Structure Visualization, Version 3.1f, Crystal Impact, Brandenburg & Putz, Bonn, **2008**.

Received: October 4, 2011

Revised: February 1, 2012

Published online: ■ ■ ■, 2012

Ready, steady, go! Chemists working on drug molecules would benefit from being able to predict the likelihood of successes or failures in salt or co-crystal formation to prioritise experimental work. We have used the hydrogen bond propensity method (see figure) to predict the success of ten molecular adduct crystallisation reactions. The results show good agreement with the experimental observations.



Hydrogen Bonds

*A. Delori, P. T. A. Galek, E. Pidcock, W. Jones** ■■■■-■■■■

Quantifying Homo- and Heteromolecular Hydrogen Bonds as a Guide for Adduct Formation 